Journal of Engineering and Applied Sciences
MEDWELL PUBLICATIONS

Dam Crack Analysis using the Fracture Mechanics Approach

Saeid Yekkebash and Vahid Yazdani
Department of Civil Engineering, Torbat-e Heydarieh Branch, Islamic Azad University, Tehran, Iran

Key words: Concrete dam, stress intensity factor, crack propagation, fracture mechanics

Corresponding Author:
Saeid Yekkebash
Department of Civil Engineering, Torbat-e Heydarieh Branch, Islamic Azad University, Tehran, Iran

Page No.: 3684-3696
Volume: 15, Issue 22, 2020
ISSN: 1816-949x
Journal of Engineering and Applied Sciences

Abstract: The present study, with the aim of applying the principles and criteria of the linear elastic fracture mechanics has investigated crack propagation in the body and foundation of a concrete gravity dam under the worst loading condition including the extraordinary loading caused by the occurrence of earthquake under full reservoir conditions. Based on the results of the analysis of fatigue crack growth in different areas of the dam, the maximum crack length is related to the area around the upper gallery, the right side of the dam and the right wall of the tunnel and in the horizontal direction. Further, the maximum amount of crack growth is related to the vertical direction and is equal to 3.15 m which has occurred under model No. 6 related to the middle of the upstream wall of the dam and the area behind the lower gallery. The results demonstrated that the amount of toughness is 2.36 in all submodelsand only in submodel No. 12, the amount of toughness equals 1.29. The stress coefficients calculated by energy and CTOD methods are not much different and in most cases, the amount of the final stress intensity factor is higher in the CTOD method. According to the obtained results and with regard tomaximum stress intensity factors, critical areas in the dam were relatively identified to be the submodel of the dam-foundation joint, submodel of the area around the lower gallery in the middle of the upstream wall of the dam, submodel of the area around the lower gallery, the right wing and the left wall of the tunnel, submodel ofcracks in the stone foundation and submodel ofthe area around the lower gallery, the left wing and the right wall of the tunnel.

INTRODUCTION

One of the most important dangers that threatens the stability of a concrete dam and may even lead to dam failure and endanger the lives of many people is to create cracks in the body of concrete dams and its growth and propagation in different directions. Due to the sensitivity of the issue of cracking in concrete dams and the inaccuracy of conventional methods that cannot accurately predict the extent of crack propagation in concrete dams and also considering the high incidence of dam cracking, today investigating the causes of cracks

and predicting their propagation have become one of the principles of determining the safety of such structures through the provision of powerful computational methods and sufficient laboratory information about the behavior of concrete during failure[1]. In failure analysis, two criteria of energy and stress intensity factor are applied[2]. In the first case, the energy criterion of crack propagation occurs when the necessary energy for the growth of the crack and the dominance over the strength of the material is provided. In other words, this feature is the energy release rate (G) reaching its critical value (G_c). Material resistance to failure (G_c), like its yield stress can be obtained through experiments and testing. In the second criterion, i.e., stress intensity factor, the failure of the object begins when its stress intensity factor (K_I, K_{II}, K_{III}) reaches the critical value of the stress intensity factor (K_{Ic}, K_{IIc}, K_{IIIc}). Subscripts I, II and III show the three modes of stress applied to the crack. In mode I, the presence of stresses perpendicular to the crack axis causes crack mouth opening. In this mode, the displacement of the crack surfaces is perpendicular to the crack surface. In mode II, shear stresses act along the crack surface and the displacement of the crack surfaces is at the surface and perpendicular to its outer edge. Shear stresses perpendicular to the plane cause the crack surfaces to be displaced at the crack surface but perpendicular to its side edge. Mode III or rupture indicates this behavior of the crack. Usually, the growth of non-critical cracks continues until the crack reaches a critical value due to the existing crack or discontinuities which ultimately leads to failure[3, 4].

The CTOD (Crack Tip Opening Displacement) method is an indicator for expressing plastic strain. Failure occurs if the CTOD exceeds a critical value. This criterion was first proposed by WELLS[5] and can be used in crack growth analysis and in cases where the crack tip plastic zone size is larger than the crack length and the LEFM theory is not applicable. By considering a central crack of length 2a, the value of the Crack Opening Displacement (COD)[6] is calculated[4, 7]. But the energy or J-integral method is a great success in the field of fracture mechanics, so that, it is a characteristic parameter of failure for nonlinear materials. By idealizing the elastic-plastic deformation with nonlinear elastic behavior, a basis for the development of fracture mechanics has been provided[8].

The Paris law[9] first proposed an equation in 1962 which relates the crack growth rate in return for increasing loading-unloading cycles directly to changes in the crack stress intensity factor[2]. Therefore, whenever the theory of fracture mechanics is used to analyze the crack behavior, it is easy to comment on the fatigue life of the analyzed structure by using Paris law and having coefficients of n and c. Studies suggest that cracks have a specific opening and closing process with respect to seasonal changes in temperature[10]. One of the important reasons for the failure and destruction of structures is the propagation of cracks and the initial defects in them. These initial cracks which are caused by various factors such as the defective process of manufacturing the structure/part, applied loads, etc., appear in different sizes and shapes in the structure and will behave differently under different loads. Some of these defects do not harm the performance of the structure while others will spread and cause a sudden and catastrophic failure of the structure. Fracture mechanics investigates the effects of these initial cracks on the responses of the structure under load and answers the following questions[9].

Since, the late 1990s, the World Tall Dams Association has approved the linear fracture mechanics method for controlling the stability and predicting the cracking of concrete dams and since, then, a number of concrete gravity dams in the United States, all built in 1930 were re-examined. Moreover, a number of important dams in the world that were damaged by various earthquakes were successfully modeled using this method in order to confirm the efficiency and reliability of this method in correctly predicting the cracking and failure of dams. The present paper has been prepared with the aim of introducing the fracture mechanics method and its application in the analysis of crack propagation in concrete dams and for the first time addresses the control of cracking in the body and foundation of one of the existing concrete dams in the country through static and dynamic analysis methods.

MATERIALS AND METHODS

The present study has performed an analysis of Kalat concrete gravity dam located in the north of Mashhad in Kalat County and at a geographical longitude of 59°54' E and a latitude of 36°43 (Fig. 1).

Materials used: The concrete of the dam body is assumed as an elastic and homogeneous material because according to the initial estimates, the stresses inside the dam body and the foundation are low and are in the elastic range. Physical and mechanical properties of the dam body concrete have been provided in Table 1. The properties of the stone foundation which is assumed to be elastic and homogeneous due to the mentioned reason, have been presented according to the three-dimensional report of the concrete dam in Table 1.

Dam analysis: Three-dimensional analysis of the dam was carried out using the finite element numerical method and Abaqus software. For this purpose, the three-dimensional geometry of the structure was modeled according to the specifications and dimensions in the

Table 1: Strength and mechanical properties of the desired dam materials

Material types	Specific gravity (γR) (kg m^{-3})	Static modulus of elasticity (E_R) (2.1E10)^{pa}	Poisson's ratio (υ)
Dam body concrete	2400	1	0.17
Stone foundation	2660	2	0.20

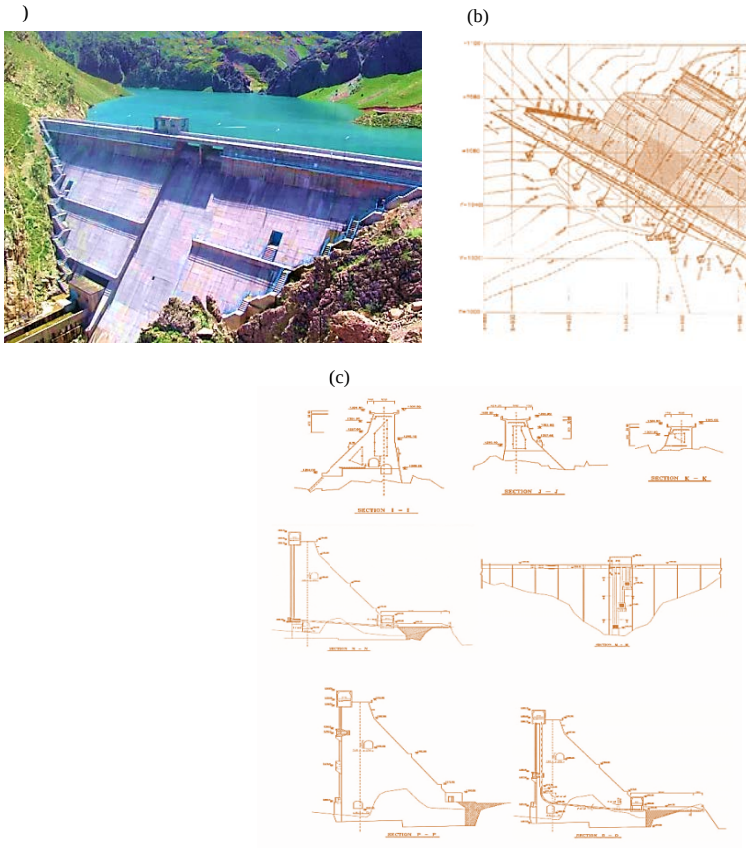

Fig. 1(a-c): Kalat concrete gravity dam located in Kalat county

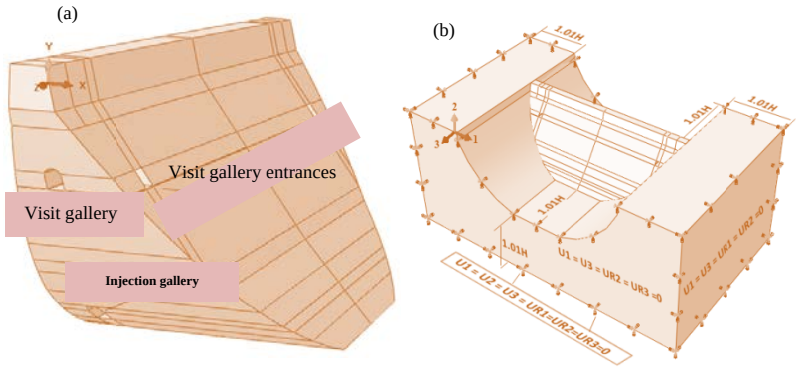

Fig. 2(a, b): (a) Three-dimensional geometry of Zavin Dam body and (b) The stone boundaries around Zavin Dam and the boundary conditions governing the problem (H, U and UR are, respectively, the dam height, the displacement in the direction of the axis and the rotation around the desired axis)

maps using Abaqus software as in Fig. 2a. Since, placing the abutment at the bottom of the dam body causes intense stress concentration in these points and gives incorrect answers about the values of stresses in the area around the abutment, part of the foundation under the dam was also modeled along with the dam, so that, the

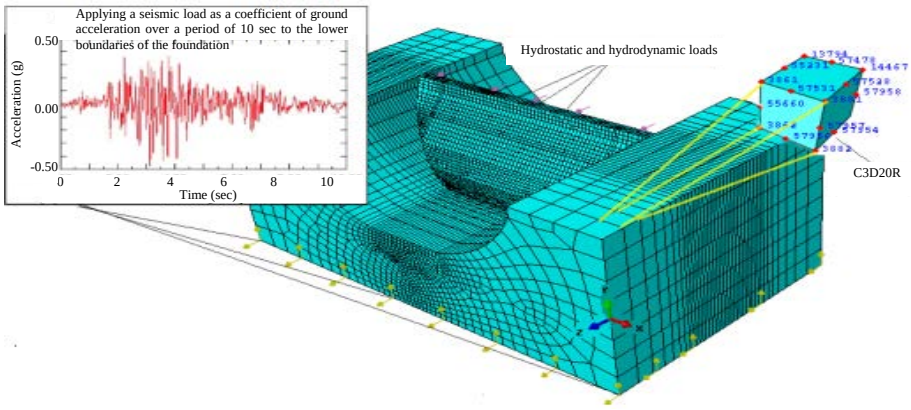

Fig. 3: Three-dimensional model mesh distribution and application of desired loads

abutment conditions were applied to the end parts of the foundation and the deformation of the abutment did not affect the stresses created in the dam body. According to the recommendations of the authorities[11-13], the area of the foundation under the dam was selected at most as much as the height of the dam from the sides of the dam body and the same size downwards and thus, the area of stone boundaries around the dam 1.01 times as much as the height of the dam from both sides and the same size in the direction of the foundation depth were modeled. Figure 2b displays the dimensions of the stone boundaries around the dam and also the boundary conditions governing the problem.

Fundamentals of the numerical method: In this study, fatigue life prediction and three-dimensional simulation of fatigue crack growth have been performed by Abaqus and Zencrack software based on the finite element method. In Zencrack software, for numerical analysis of fatigue crack, the parameters of fracture mechanics (stress intensity factor K_I and energy release rate G) were measured based on CTOD and Energy methods[6].

Applying loads to the dam and meshing the model: Here, the force caused by the upstream sediment pressure is not considered due to its insignificant effects on the amount of stresses created in the dam body. Besides, due to the condition of the area, the dam location and the small surface of the dam reservoir lake, the effects of wind force, wave force and ice force were disregarded. Because of the great thickness of the dam, the effects of temperature and thermal stress sensitivity have been reduced[14]. Therefore, the effect of temperature change was also ignored. In order to analyze the dam against the combined earthquake, the following loads were considered in the modeling. The hydrostatic force of water at normal level was considered as an extensivenodal load (length/force) perpendicular to the surface of the upstream body at the dam-foundation joint. Further, the weight of the dam in the form of linear acceleration in the opposite direction of the y-axis and the inertial force exerted on the dam body due to ground acceleration was applied in the form of variable accelerations in a period of 10 sec in the horizontal directions and perpendicular to the boundaries of the dam foundation according to the provided accelerometer (one of the recent earthquakes in the north of Khorasan Province) (Fig. 3). Additionally, hydrodynamic force caused by the effect of earthquake on the volume of water in the reservoir was appliedthrough the proposed USBR method with quadratic distribution (parabolic) and perpendicular to the upstream body of the dam, from zero at normal level to its maximum value at the bottom of the dam. The dam body and its foundation were meshed separately using C3D20R second-order twenty-node hexahedral brick elements (Fig. 3). The dimensions of the mesh elements of the dam body were considered smaller than the stone border elements due to their importance. On the other hand, in order to maintain the accuracy of the analysis and also to reduce the volume of calculations, the dam foundation meshing was done radially, so that, at the stone boundaries by approaching the body of the dam, the dimensions of the elements will be smaller.

Analysis of the dam: After building the model and assigning the material specifications to the model and applying the loads and boundary conditions governing the problem, numerical analysis of the structure (finite elements) was performed by Abaqus software with dynamic relaxation method. For dynamic analysis of the dam, an explicit method was used which is specific to the dynamic analysis of large models (dam) with short dynamic time responses (earthquake). The results of the initial analysis of the dam model and its foundation (without cracks) under a combination of the above loadings using Abaqus software are shown in Fig. 4a, b. These figures display how the compressive and tensile stresses are distributed in the dam body.

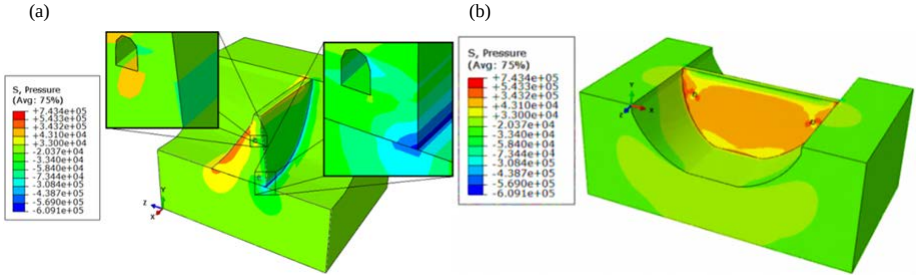

Fig. 4(a, b): Distribution of maximum compressive and tensile stresses with a full reservoir under seismic loading and (b) Distribution and location of maximum tensile stresses created in a dam with a full reservoir under seismic loading

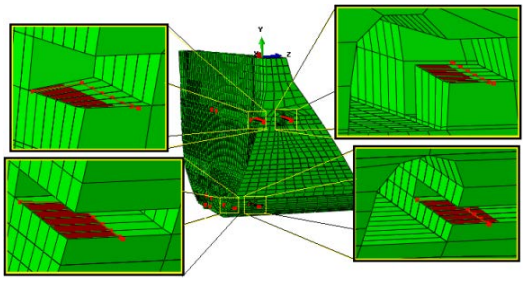

Fig. 5: Location of four initial cracks considered on the right wing of the model

Initial cracks in the dam cross section: Almost the entire dam body, except for a small area on the wings and heel of the dam (where the dam connects to the foundation), the wall and the floor of both the lower and upper galleries are under compressive stresses. Hence, in the points under tension, the initial crack with a length equal to the length of the area under tension was considered. Based on the foregoing, 12 initial cracks (4 on the right wing, 4 on the left wing and 4 in the middle and heel of the upstream wall of the dam) at a depth of 1 m along the z-axis (except for one case at a depth of 2 m along the y-axis) and with a length of 6 m along the x-axis (except for two cases with a length of 8 m) at points under tension were considered with the help of Zencrack software (Fig. 5) and for each crack, fatigue crack analysis was performed separately.

Fatigue crack analysis in the desired dam under seismic load: The following submodeling process used in dam analysis was performed as follows:

Creating and analyzing a general model: First, the general model of the dam, also called the "coarse-grained model", was created and analyzed and the areas under considerable tension were identified.

Creating a submodel with more details: After identifying the areas under tension and determining the location of the initial cracks (12) in the dam model, the submodel related to the area around each crack was created and carefully meshed by adding more details. It should be noted that the number of submodels of the problem was considered with respect to the number of initial cracks considered in the dam model, i.e., 12.

Performing interpolation for the truncated boundary: Boundary conditions were created on the truncated boundary by interpolating the results of the general model on the truncated boundary of each submodel. In other words, the effect of other parts of the model acts as boundary conditions (usually displacement boundary conditions) on the truncated boundaries.

Analyzing the submodel: By applying the truncated boundary conditions, all submodels were re-analyzed without considering the crack. The results of the submodel analysis were compared with the results of coarse-grained model and were highly consistent. After analyzing and ensuring the consistency of the results of each submodel with the results of the corresponding location in the general model of the dam, the uncracked meshed model of each submodel was introduced to the Zencrack fracture mechanics code and the location of the dimensions of initial cracks in each submodel was determined using Zencrack software.

Fatigue data: First of all, it should be noted that among the loads applied to the dam model, only the hydrodynamic loads and the seismic load are variable during the analysis period and unlike gravity and hydrostatic loads which are cyclic with variable amplitude, these two cyclic loads (seismic load and hydrodynamic load) provide the ground for the creation of fatigue phenomenon and crack growth in the dam model. According to the accelerometer of Fig. 6, during the earthquake, the forces caused by the earthquake will be variable following the accelerations due to the variability of the accelerations applied to the lower boundaries of the model. In order to make the variable accelerations cyclic, one of the cycle counting methods called rain-flow-counting algorithm was used. To this end, the

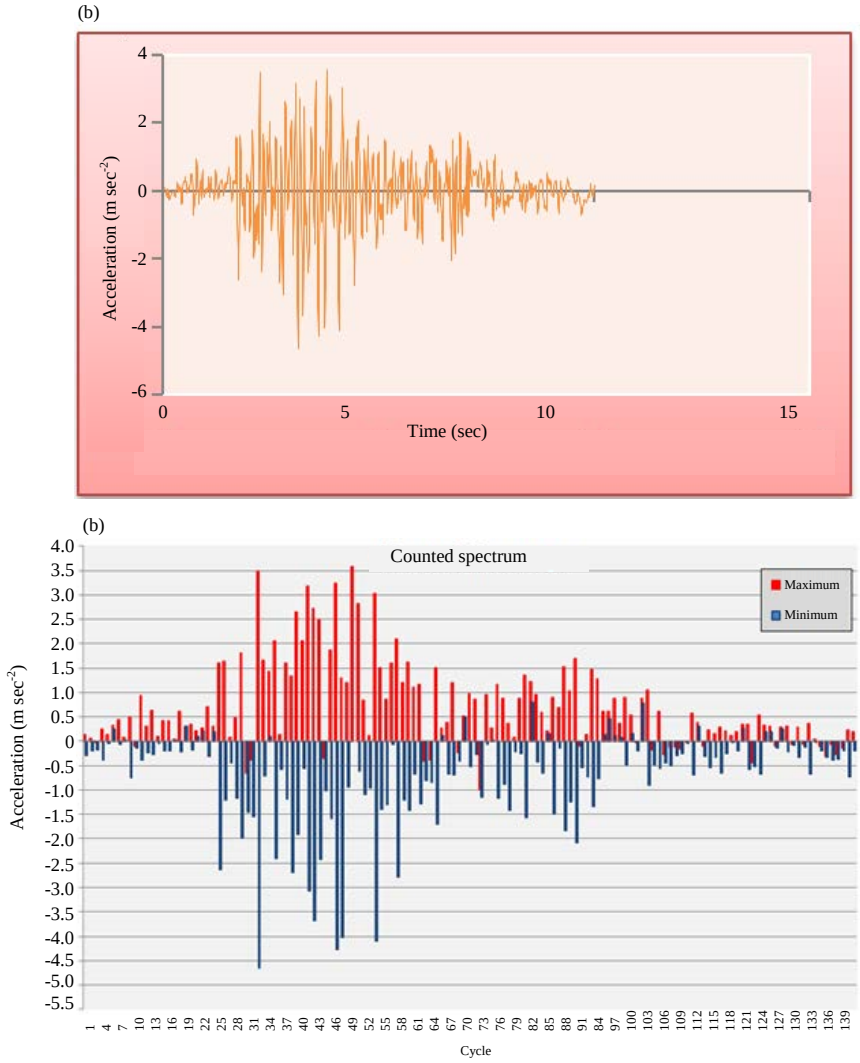

Fig. 6(a, b): (a) Earthquake-induced horizontal accelerometer diagram and (b) Acceleration cycle diagram using rain-flow algorithm

accelerometer data provided as a coefficient diagram of acceleration-time was initially drawn as a acceleration-time graph (Fig. 6). Then, the data in the diagram which contains 999 data lines were introduced to the rain-flow program and based on this algorithm, the acceleration-time data were converted to acceleration cycle. As provided in Fig. 6 by applying this algorithm, the total earthquake time history is converted to 139 cycles, each having its own maximum and minimum acceleration values.

After performing the cycle counting process, static and cyclic loads with variable amplitude were applied to the dam model simultaneously using Zencrack software and the relevant coding and after preparing the cracked meshed model (cracked submodel), considering the use of Paris law and the calibration constants (Paris constants) used in the software, i.e., c and n, for the stone boundaries and the concrete body of the dam and also to evaluate the stability of the dam and analyze the final results, plane strain fracture toughness (critical stress intensity factor K_{Ic}) of dam materials and stone foundation around the dam were used. Based on the proposal by Galvez *et al.*[12] and as quoted by Kishen and Singh[15], fracture toughness of the dam concrete and foundation stone materials were considered $K_{IC} = 2.3E6Pa\sqrt{m}$ and $K_{IC} = 1.29E6Pa\sqrt{m}$, respectively and finally, the fatigue crack growth analysis code was written for each submodel and the problem analysis was performed.

RESULTS AND DISCUSSION

Results of numerical analysis of fatigue crack growth in Zavin dam: After applying a combination of different

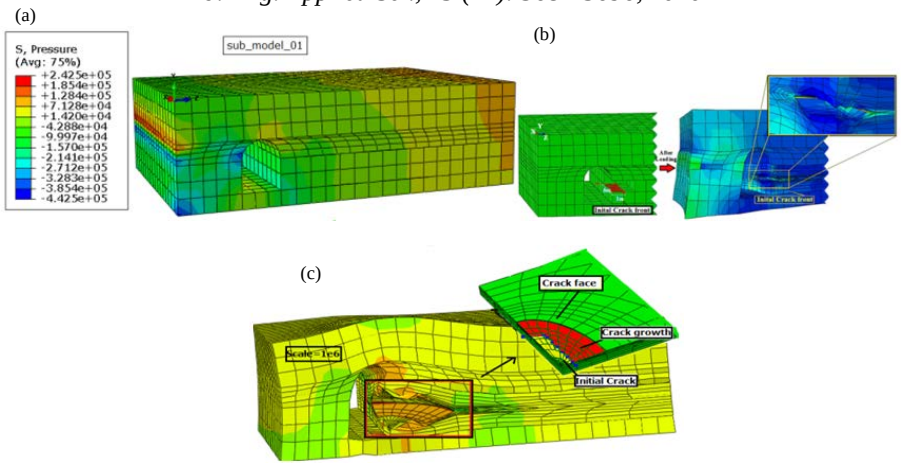

Fig. 7(a-c): (a) Submodel No. 1 of the area under study, (b) Display of initial crack in submodel No. 1 (before and after the first loading) and (c) Display of fatigue crack growth in subm-odel No. 1 (display scale: 1e6)

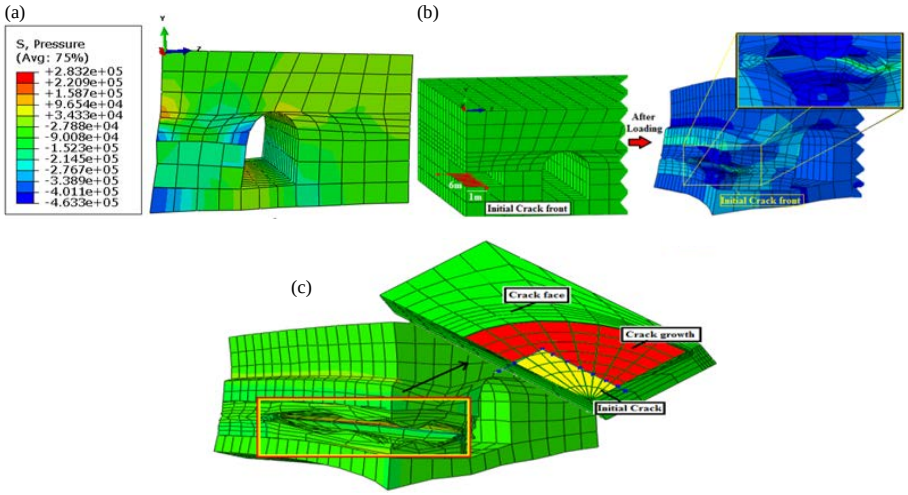

Fig. 8(a-c): (a) Submodel No. 2 of the area under study, (b) Display of the initial crack in submodel No. 2 (before and after the first loading) and (c) Display of fatigue crack growth in submodel No. 2 (display scale: 1e6)

loads to the dam model, considering the initial cracks in areas of the dam where there is a potential for cracking, the results of analysis of each submodel (without cracks), the initial crack location and fatigue crack growth in each submodel and crack length diagrams versus stress intensity factors obtained from fatigue crack analysis for all submodels under study have been displayed in Fig. 7- 17.

Submodel No. 1: This submodel is related to the area around the lower gallery, the right side of the dam and the right wall of the tunnel and the results of its analysis are as follows:

Submodel No. 2: This submodel is related to the area around the lower gallery, the right side of the dam and the left wall of the tunnel and the results of its analysis are as follows:

Submodel No. 3: This submodel is related to the area around the upper gallery, the right side of the dam and the right wall of the tunnel and the results of its analysis are as follows:

Submodel No. 4: This submodel is related to the area around the upper gallery, the right side of the dam and the left wall of the tunnel and the results of its analysis are as follows:

Submodel No. 5: This submodel is related to the middle of the upstream wall of the dam and the area behind the upper gallery and the results of its analysis are as follows:

Submodel No. 6: This submodel is related to the middle of the upstream wall of the dam and the area behind the lower gallery and the results of its analysis are as follows:

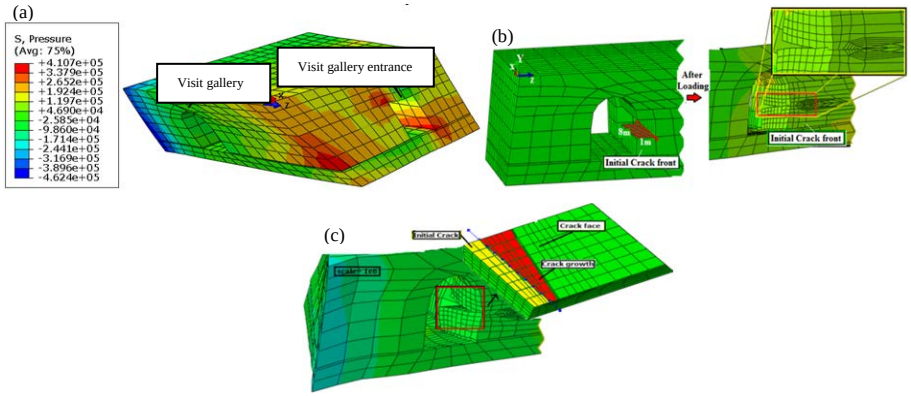

Fig. 9(a-c): (a) Submodel No. 3 of the area under study, (b) Display of the initial crack in submodel No. 3 (before and after the first loading) and (c) Display of fatigue crack growth in submodel No. 3 (display scale: 1e6)

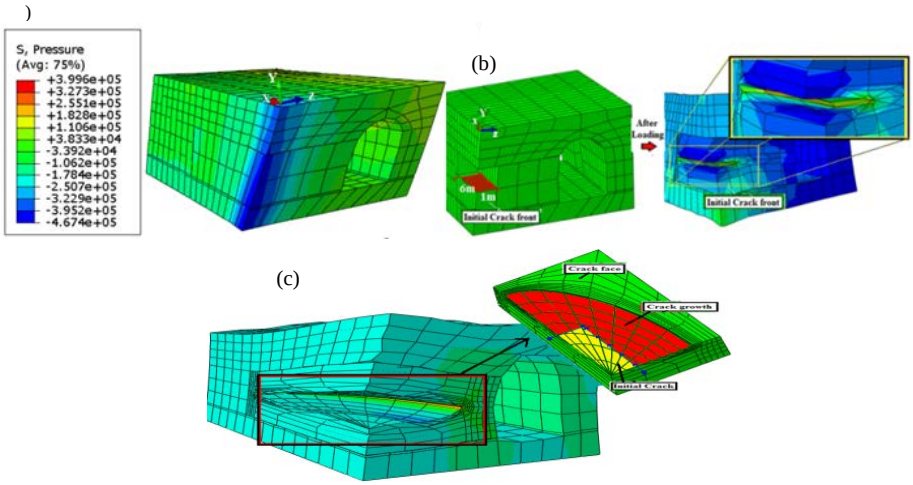

Fig. 10(a-c): (a) Submodel No. 4 of the area under study, (b) Display of the initial crack in submodel No. 4 (before and after the first loading) and (c) Display of fatigue crack growth in submodel No. 4 (display scale: 1e6)

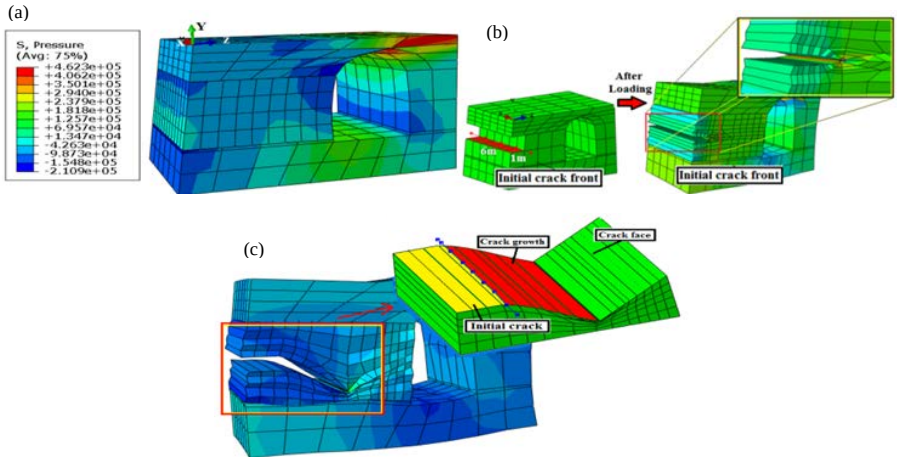

Fig. 11(a-c): (a) Submodel No. 5 of the area under study, (b) Display of the initial crack in submodel No. 5 (before and after the first loading) and (c) Display of fatigue crack growth in submodel No. 5 (display scale: 1e6)

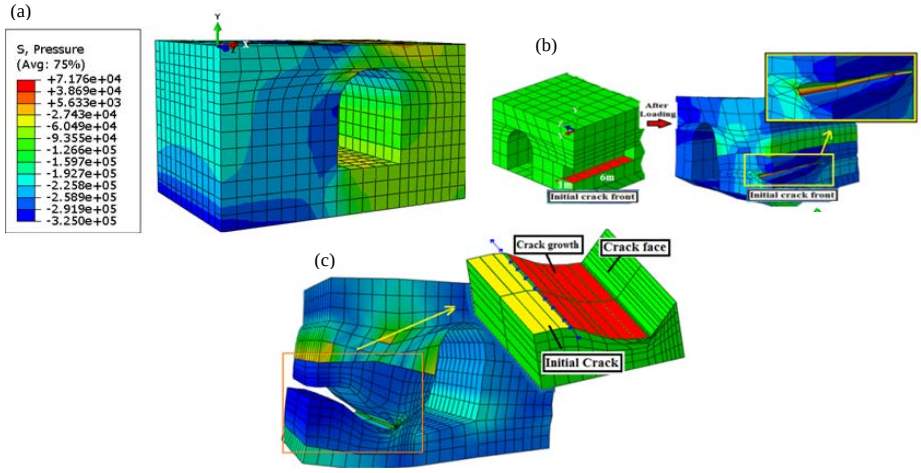

Fig. 12(a-c): (a) Submodel No. 6 of the area under study, (b) Display of the initial crack in submodel No. 6 (before and after the first loading) and (c) Display of fatigue crack growth in submodel No. 6 (display scale: 1e6)

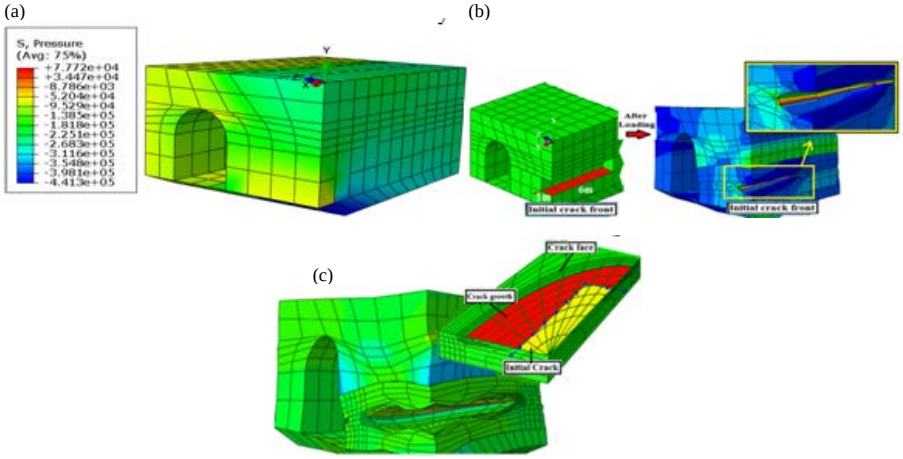

Fig. 13(a-c): (a) Submodel No. 7 of the area under study, (b) Display of the initial crack in submodel No. 7 (before and after the first loading) and (c) Display of fatigue crack growth in submodel No. 7 (display scale: 1e6)

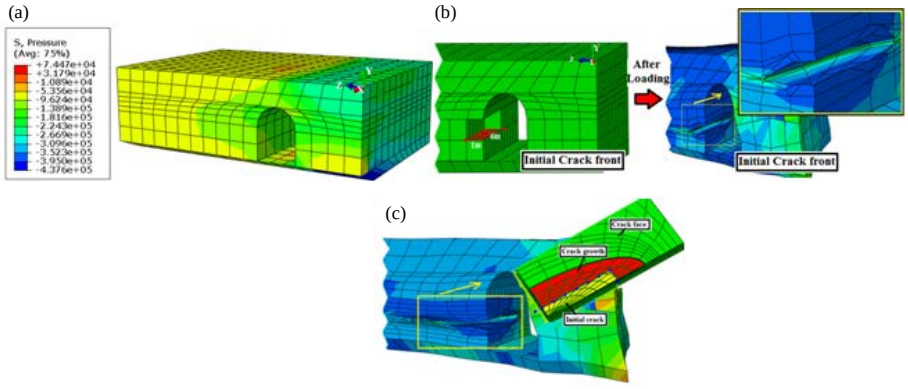

Fig. 14(a-c): (a) Submodel No. 8 of the area under study, (b) Display of the initial crack in submodel No. 8 (before and after the first loading) and (c) Display of fatigue crack growth in submodel No. 8 (display scale: 1e6)

Submodel No. 7: This submodel is related to the area around the lower gallery, the left side of the dam and the right wall of the tunnel and the results of its analysis are as follows:

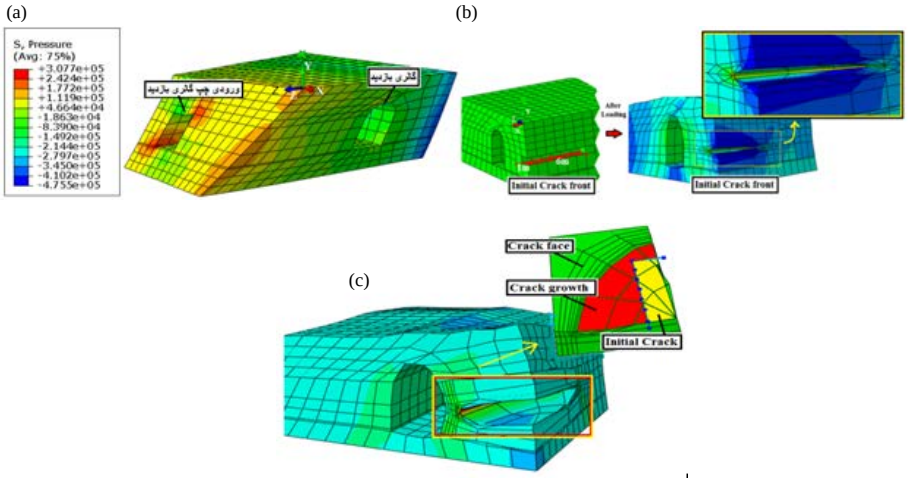

Fig. 15(a-c): (a) Submodel No. 9 of the area under study, (b) Display of the initial crack in submodel No. 9 (before and after the first loading) and (c) Display of fatigue crack growth in submodel No. 9 (display scale: 1e6)

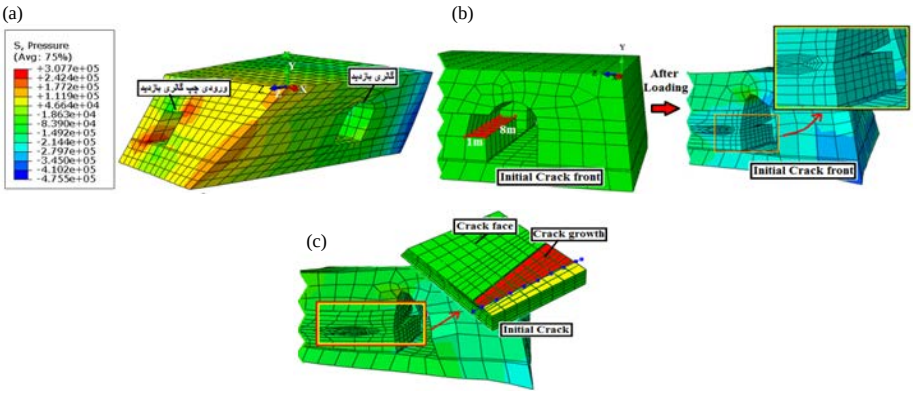

Fig. 16(a-c): (a) Submodel No. 10 of the area under study, (b) Display of the initial crack in submodel No. 10 (before and after the first loading) and (c) Display of fatigue crack growth in submodel No. 10 (display scale: 1e6)

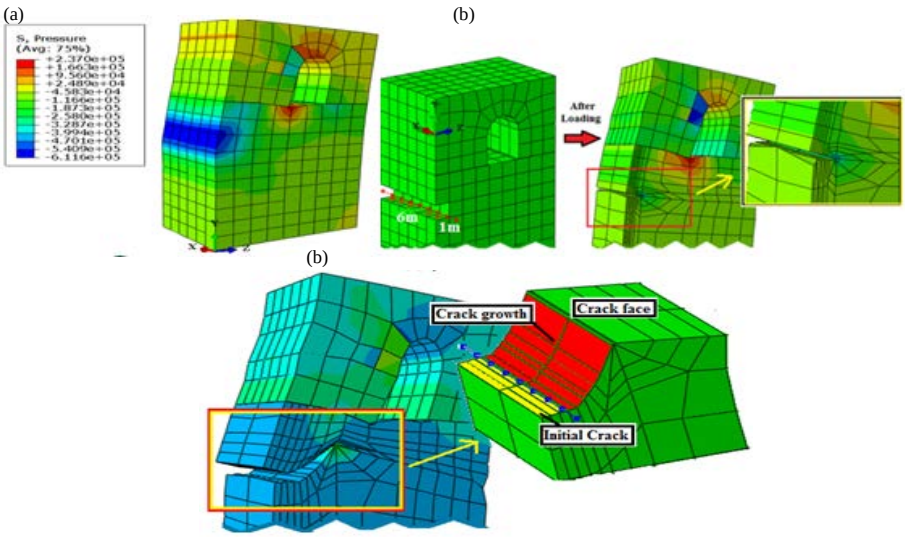

Fig. 17(a-c): Submodel No. 11 of the area under study, (b) Display of the initial crack in submodel No. 11 (before and after the first loading) and (c) Display of fatigue crack growth in submodel No. 11 (display scale: 1e6)

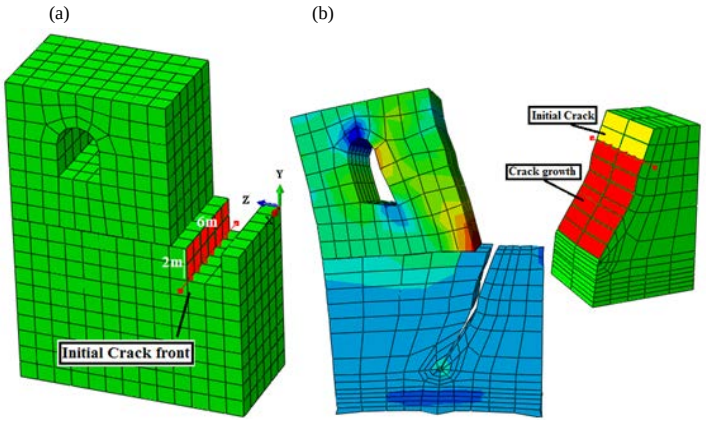

Fig. 18(a, b): (a) Submodel No. 12 of the area under study and (b) Display of fatigue crack growth in submodel No. 12 (display scale: 1e6)

Table 2: Results of fatigue crack growth analysis in different areas of the dam

Initial crack location	Initial crack length in different directions (m)			Crack growth rate in different directions (m)			Final stress intensity factor $Pa\sqrt{m}$ (K_I)		Material fracture toughness
Submodel	X	Y	Z	X	Y	Z	Energy method (E6)	CTOD method (E6)	(K_{IC}) $Pa\sqrt{m}$ (E6)
1	6	-	1	2.5	-	2.51	0.852	0.8530	2.36
2	6	-	1	2.5	-	3.01	0.996	0.9960	2.36
3	6	-	1	-	-	1.98	0.669	0.6701	2.36
4	6	-	1	2.3	-	2.00	0.809	0.8090	2.36
5	6	-	1	-	-1.6	2.50	0.708	0.7090	2.36
6	6	-	1	-	-2	3.15	1.091	0.7090	2.36
7	6	-	1	3	-	3.06	0.878	1.0910	2.36
8	6	-	1	2	-	2.70	0.808	0.8790	2.36
9	6	-	1	1.8	-	2.11	0.769	0.8090	2.36
10	6	-	1	-	-	2.51	0.7132	0.7700	2.36
11	6	-	1	-	3.08	2.50	1.159	0.7140	2.36
12	6	1	-	-	-3.9	2.30	0.952	1.1590	1.29

Submodel No. 8: This submodel is related to the area around the lower gallery, the left side of the dam and the left wall of the tunnel and the results of its analysis are as follows:

Submodel No. 9: This submodel is related to the area around the upper gallery, the left side of the dam and the right wall of the tunnel and the results of its analysis are as follows:

Submodel No. 10: This submodel is related to the area around the upper gallery, the right side of the dam and the left wall of the tunnel and the results of its analysis are as follows:

Submodel No. 11: This submodel is related to the area of the dam body-foundation joint and the middle of the upstream wall and the results of its analysis are as follows:

Submodel No. 12: This submodel is the same as submodel No. 11 but with a vertical crack in the stone foundation and the results of its analysis are as follows (Fig. 18).

Graphs of stress intensity factor vs. crack length of submodels: Stress intensity factor-crack length graphsrelated to submodels are shown in Fig. 19a-d. The relevant graphs are drawn after transferring the numbers obtained from crack analysis in Excel. In the above figures, the horizontal axis is the crack length (m) and the vertical axis is the stress intensity factor ($Pa\sqrt{m}$).

Final results of fatigue crack growth analysis: Based on the results of fatigue crack growth analysis in different areas of the dam (Table 2), the maximum crack length is related to submodel No. 3, i.e., the area around the upper gallery, the right side of the dam and the right wall of the tunnel and in the horizontal direction. Moreover, the highest amount of crack growth is related to the vertical direction and is equal to 3.15 m which has occurred in submodel No. 6 related to the middle of the upstream wall of the dam and the area behind the lower gallery. The results revealed that the amount of toughness in all submodels is equal to 2.36 and only in submodel No. 12 (the same as submodel No. 11 but with a vertical crack in the stone foundation), the amount of toughness is equal to 1.29. As shown in Table 2, the value of the stress

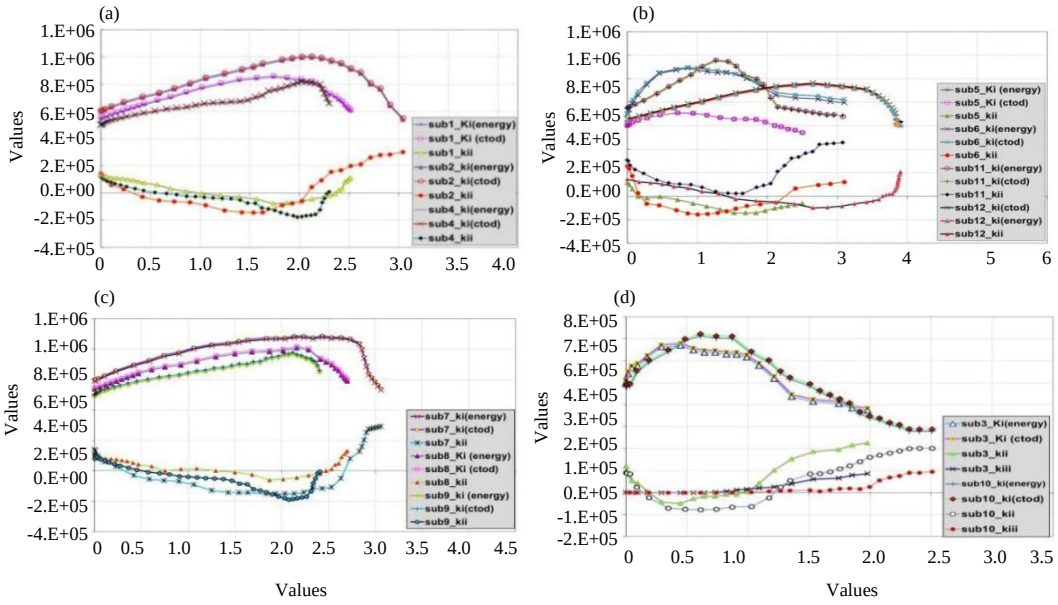

Fig. 19(a-d): Submodels of the dam, (a) the right wing of the dam, (b) the middle to the upstream wall, (c) the left wing of the dam and (d) Two visit gallery entrances

coefficient calculated by energy and CTOD methods are not much different and in most cases, the value of the final stress intensity factor is higher in the CTOD method.

CONCLUSION

The results demonstrated that in the studied dam under seismic load in a period of 10 sec, the maximum tensile and compressive stresses have occurred in a period of 2.32-4.26 sec. On the other hand, due to the great importance of tensile stresses, points such as the body-foundation joint and the floor and the wall of both the visit and injection galleries were under tensile stresses more often during the earthquake.

According to the obtained results, crack growth in all areas adjacent to the dam wings is in the form of a plane that has extended only along the longitudinal and transverse axes. But by moving away from the wings and towards the center of the dam, the crack growth has no longer the shape of a plane and has also extended along the vertical axis (in the same direction and in the opposite direction of this axis). The reason for this issue (the crack growth being in the shape of a plane on the lateral boundaries of the dam) is the impact of the abutments of the dam wings. Considering the values of the relevant stress intensity factors in the studied areas, the dominant mode of crack growth in different areas of the dam can be the first mode, i.e., the opening mode, so that, there is a significant difference between the values of stress intensity factors of the first mode (K_I) and other modes (K_{II} and K_{III}). It is noteworthy that with increased crack growth, the stress intensity factors of the first mode (K_I) after reaching the final value have decreased and the values of the second mode (K_{II}) have been added and the second mode has been finally, effective in crack growth. Investigations have determined that the values of stress intensity factors of the third mode (K_{III}) in all the studied areas were close to zero and had no role in the type of crack growth except inthe areas of upper gallery entrances (visit gallery entrances) where in addition to the first and second modes, a significant rupture mode is also seen in crack growth. The reason isthe effect of abutments of the wings (the restrictive role of crack growth) and the presence of a free surface in these entrances. By comparing the amount and direction of crack growth in different areas of the dam, it can be found that in all areas under study by moving away from the crest and approaching the foundation, crack growth has also increased following the increase in tensile stresses and the highest crack growth in the dam body has occurred at the dam-foundation joint and the surrounding areas and the highest crack growth in the whole structure has occurred in the stone foundation of the dam with an initial vertical crack and along the transverse axis. By moving away from the wings and approaching the center of the dam, the crack growth limit has decreased and the crack has also extended along the vertical axis (in submodels related to the middle of the upstream wall of the dam, the area behind the upper gallery, the middle of the upstream wall of the dam, the area behind the lower gallery, dam body-foundation joint and the middle of the upstream wall but with a vertical crack in the stone foundation). It

should be noted that in the submodels related to the areas around the visit gallery entrances, crack growth along the transverse axis with two values indicates the same thing due to the simultaneous effect of the second and third modes in these areas so thatthe minimum growth values are related to the crack advance towards the wings and the growth restriction and the maximum growth values are related to the crack advance near the free surface of these entrances. As previously mentioned, stress intensity factors were determined during crack analysis in the dam using CTOD and energy methods and with regard to the predominance of the opening mode in most areas, the maximum stress intensity factors related to this mode (K_I) were presented. As can be observed, the results of these two methods (CTOD and Energy) are close to each other and are acceptable.

According to the diagram related to the submodel of the dam body-foundation joint and the middle of the upstream wall but with a vertical crack in the stone foundation, a big difference can be seen between the results of this submodel and other results whose reason can be the different materials of this area (stone foundation) compared to other areas (concrete). After crack analysis, in order to determine the critical areas in terms of dam stability, the maximum stress intensity factors of the first mode in each submodel with the plane strain fracture toughness of the material containing the crack were compared. As can be seen in all the studied areas in the dam body, the final stress intensity factors are lower than the fracture toughness of the dam concrete $(Pa\sqrt{m}2)$ and similarly, the maximum stress intensity factors resulting from crack growth in the foundation are less than the fracture toughness of the dam stone foundation. Consequently, they cannot be problematic in terms of the stability of the dam under study. Critical areas in the studied dam were identified relatively or according to the maximum stress intensity factors as the following: Submodel of the dam-foundation joint, submodel of the area around the lower gallery and the middle of the upstream wall of the dam, submodel of the area around the lower gallery and the right wing and the left wall of the tunnel, submodel of the crack in the stone foundation and submodel of the area around the lower gallery, the left wing and the right wall of the tunnel).

REFERENCES

01. Linsbauer, H.N., 1990. Design and Construction of Concrete Dams Under Consideration of Fracture Mechanics Aspects. In: Analysis of Concrete Structures by Fracture Mechanics, Elfgren, L. and S.P. Shah (Eds.)., CRC Press, Boca Raton, Florida, pp: 155-162.
02. Paris, P.C., M.P. Gomez and W.E. Anderson, 1961. A rational analytic theory of fatigue. Trend Eng., 13: 9-14.
03. Schijve, J., 2009. Fatigue of Structures and Material. 2nd Edn., Springer, Berlin, Germany,.
04. Socie, F., 2009. Fatigue and Fracture. University of Illinois, Illinois, USA.,
05. EPRI., 2002. Theory manual. MERLIN-2, Version 2.0. Electric Power Research Institute, Washington, USA.
06. Zencrack, 2011. Background and theory manual. Zentech Inc., Houston, Texas.
07. Meguid, S.A., 1989. Engineering Fracture Mechanics. Elsevier Applied Science Publishers, England, UK.,.
08. Broek, D., 1986. Elementary Engineering Fracture Mechanics. 4th Edn., Martinus Nijhoff Publishers, Netherlands.
09. Shah, S.P., S.E. Swartz and C. Ouyang, 1995. Fracture Mechanics of Concrete: Applications of Fracture Mechanics to Concrete, Rock and Other Quasi-Brittle Materials. John Wiley & Sons Inc, Hoboken, New Jersey,.
10. United State Bureau of Reclamation, 1976. Design of Gravity Dams: Design Manual for Concrete Gravity Dams Gravity. U.S. Government Printing Office, Washington,.
11. Plizzari, G.A., 1997. LEFM applications to concrete gravity dams. J. Eng. Mech., 123: 808-815.
12. Galvez, J., J. Llorca and M. Elices, 1996. Fracture mechanics analysis of crack stability in concrete gravity dams. Dam Eng., 7: 35-64.
13. Saouma, V.E. and D. Milner, 1996. On why fracture mechanics should be adopted for dam safety investigation. Dam Eng., 7: 215-231.
14. Abrishami, J. and N.V. Rajaee, 2001. Concrete Dams Design and Construction. 1st Edn., Astan Quds Razavi Publications, Tehran, Iran,.
15. Kishen, J.C. and K.D. Singh, 2001. Stress intensity factors based fracture criteria for kinking and branching of interface crack: Application to dams. Eng. Fract. Mech., 68: 201-219.